# Integrating dynamical modeling and phylogeographic inference to characterize global influenza circulation

Francesco Parino[a,1], Emanuele Gustani-Buss[b,1], Trevor Bedford[c,d], Marc A. Suchard[e,f], Nídia Sequeira Trovão[g], Andrew Rambaut[h], Vittoria Colizza[a,i,2], Chiara Poletto[j,2,3], and Philippe Lemey[b,2,3]

[a]Sorbonne Université, INSERM, Institut Pierre Louis d'Epidemiologie et de Santé Publique (IPLESP), Paris, France
[b]Department of Microbiology, Immunology and Transplantation, Rega Institute, KU Leuven – University of Leuven, 3000 Leuven, Belgium
[c]Vaccine and Infectious Disease Division, Fred Hutchinson Cancer Center, Seattle, Washington 98109, USA
[d]Howard Hughes Medical Institute, Seattle, Washington 98109, USA
[e]Departments of Biomathematics and Human Genetics, David Geffen School of Medicine at UCLA, University of California, Los Angeles, CA, 90095, USA
[f]Department of Biostatistics, UCLA Fielding School of Public Health, University of California, Los Angeles, CA, 90095, USA
[g]Fogarty International Center, National Institutes of Health, Bethesda, MD, USA
[h]Institute of Ecology and Evolution, University of Edinburgh, Edinburgh EH9 3FL, UK.
[i]Department of Biology, Georgetown University, Washington, DC, USA.
[j]Department of Molecular Medicine, University of Padova, 35121 Padova, Italy
[1]F.P. and E.G.-B. contributed equally to this work.
[2]V.C., C.P. and P.L. contributed equally to this work.
[3]To whom correspondence should be addressed: philippe.lemey@kuleuven.be, chiara.poletto@unipd.it

# Contents



# 1 Global Epidemic and Mobility Model

## 1.1 Data sources

GLEAM accounts for worldwide population distribution, mobility by flight, and national commuting, modeled based on the following datasets:

- **Population distribution.** Population distribution is based on high-resolution data from the 'Gridded Population of the World' project of the Socioeconomic Data and Applications Center at Columbia University [1]. Specifically, this database provides a population estimate on a grid of cells covering the whole planet at a resolution of 15×15 minutes of arc. Those cells are assigned to nearby transportation hubs by a Voronoi-like tessellation structure that takes into account distance constraints, forming geographic census areas around each hub. The present version of the model uses 3,362 of such census areas in 220 countries.

- **Air travel.** Human mobility integrates the global flight network with the short-scale daily commuting patterns between adjacent patches. In

particular, mobility by flight is modeled based on the data set provided by the International Air Transport Association and the Official Airline Guide [2] containing all worldwide origin-destination trips during 2013.

- **Commuting.** The commuting considers data from $80,000$ administrative regions from 30 countries in 5 different continents [3]. Data of different spatial resolution levels are mapped into the geographical census areas formed by the Voronoi-like tessellation procedure around the main transportation hubs. The fact that census areas are relatively homogeneous allows us to estimate a gravity law that successfully reproduces the commuting data obtained across different continents and provides us with estimates for the possible commuting levels in the countries for which such data are not available [3, 4]. The mapped commuting flows can be considered as a second transport network connecting geographically close patches.

## 1.2 Model of air-travel

### 1.2.1 Network reconstruction and traveling process

A weighted network is built from the data by assigning to each airport pair $i$, $j$ the average daily number of passengers, $w_{ij}$, traveling between the two airports during 2013. The resulting network has $\sim 670,000$ links with a total of 7 million daily passengers. The network shows a high degree of heterogeneity both in the number of destinations per airport and in the number of passengers per connection. To avoid excessive computational times (proportional to the number of mobility links) a filtered network was generated by removing links with less than 2 passengers per day, thus keeping the high-traffic links corresponding to 16% of the total links and accounting for 98% of the total traffic. As an alternative method, we tested also the disparity filter[5] for extracting the backbone of the network - i.e. a filtering procedure that preserves the edges that represent statistically significant deviations with respect to a null model for the local assignment of weights to edges. However, simple threshold-based filtering was preferred in that, despite altering the distribution of weights, it preserved the geographic repartition of travelers.

Mobility based on air travel is modeled explicitly, as a discrete-time multinomial process with the time scale of one day [6]. Daily travel flux, $w_{ij}$, are used to compute transition probabilities that rule the travel dynamics. The recurrent and the Markovian travel approaches differ in that the former assumes individuals leave their residence patch for a certain destination and then return home after a certain time, while the second considers

random traveling trajectories where the individuals have no assigned patch of residence.

### 1.2.2 Markovian travel

Individuals in the patch $i$, belonging to the disease compartment $X_i$ (among susceptible, latent, asymptomatic infectious, etc., as described in the following section), can travel to every patch $j$ of the set $\Gamma_i$ of $i$'s neighboring populations in the air-travel network. At each time step $\Delta t$, the traveling probability from $i$ to $j$ is computed as $p_{ij} = w_{ij}\Delta t/N_i$, with $N_i$ being the population of $i$. At each time step, from the probability vector $\{p_{ij}\}_{j\in\Gamma_i}$ multinomial extractions yield the number of travelers $\Delta X_{ij}$ from $i$ to $j$. Once the numbers of travelers are extracted for each connection, the occupation number of the class $X_i$ in each patch is updated according to incoming and outgoing individuals

$$X_i(t) = X_i(t-1) + \sum_{j\in\Gamma_i} \Delta X_{ji} - \Delta X_{ij}.$$

### 1.2.3 Recurrent travel

We followed the approach of [7, 8, 9, 10] here implemented in a fully stochastic individual-based version. $N_i$ individuals are assigned to the patch of residence $i$ and further subdivided into mobility classes, according to the patch where they are present at a given time. $N_{ij}(t)$ is thus the class of individuals who are resident in $i$ and traveling at time $t$ in the neighboring patch $j$, while the class $N_{ii}(t)$ groups individuals resident in $i$ and not traveling at time step $t$ – the same applies to each disease compartment $X$, in such a way that $X_{ij}(t)$ is the class of individuals in disease compartment $X$, who are resident in the patch $i$ and traveling at time $t$ in the neighboring patch $j$. At each time step $\Delta t$, individuals of each compartment $X$ leave $i$ for the destination $j$ with probability $\nu_{ij}\Delta t$ and they return to $i$ with probability $\Delta t/\tau$, with $\tau$ being the average length of stay. Following these rules, mobility classes are updated at each time step with binomial and multinomial extractions.

Model parametrization is based on air-transport data and traveling statistics as follows. The average length of stay on the travel destination, $\tau$, is assumed to be the same for every patch and equal to 15 days (i.e. return rate 1/15 days$^{-1}$) [3]. The rate of leaving, $\nu_{ij}$, is instead chosen to recover the traveling fluxes of the air-travel database. To achieve this, we assume the mobility dynamics to be at equilibrium, with the occupation numbers

of the mobility classes stable in time. These can be computed from the continuous differential equations

$$\begin{aligned} \partial_t N_{ii} = & \quad -\nu_i N_{ii}(t) + \tau^{-1} \textstyle\sum_{j\in\Gamma_i} N_{ij}(t), \\ \partial_t N_{ij} = & \quad \nu_{ij} N_{ii}(t) - \tau^{-1} N_{ij}(t), \end{aligned} \tag{1}$$

where $\Gamma_i$ is the set of $i$'s neighboring populations and $\nu_i = \sum_{j\in\Gamma_i} \nu_{ij}$. The equilibrium condition then reads

$$\begin{aligned} N_{ii} &= \frac{N_i}{1+\tau\nu_i}, \\ N_{ij} &= \frac{N_i \tau \nu_{ij}}{1+\tau\nu_i}. \end{aligned} \tag{2}$$

This implies that the daily flux of passengers along a connection, $w_{ij}$, can be computed as the sum of individuals leaving their residence patch and individuals returning home, namely

$$\begin{aligned} w_{ij} &= \nu_{ij} N_{ii} + N_{ji}/\tau \\ &= \frac{N_i \nu_{ij}}{1+\tau\nu_i} + \frac{N_j \nu_{ji}}{1+\tau\nu_j}. \end{aligned} \tag{3}$$

The equilibrium condition implies the symmetry condition $w_{ij} = w_{ji}$, in that for the node population to be stable people returning home must be equal on average to people leaving. In order to compute $\nu_{ij}$ from $w_{ij}$, we note, however, that Eq. 3 provides a degenerate system of equations with the number of equations being half of the number of variables. This is due to the symmetry condition $w_{ij} = w_{ji}$, that a priori does not hold for $\nu_{ij}$. Therefore, to compute the set of leaving rates other constraints must be assumed. Here, we assumed that the travelers are equally subdivided into people departing and people returning home, namely $\nu_{ij} N_{ii} = N_{ji}/\tau = w_{ij}/2$. A different assumption was tested ($\nu_{ij} = \nu_{ji}$) without noticeable variation in the simulated epidemic dynamics.

### 1.3 Model of transmission and commuting

Inside each patch of the metapopulation model, we consider a compartmental scheme, typical of influenza-like illnesses (ILIs), where each individual has a discrete disease state assigned at each moment in time among Susceptible, Latent, Asymptomatic Infectious, Symptomatic Infectious that can travel, Symptomatic Infectious that cannot travel due to the severity of

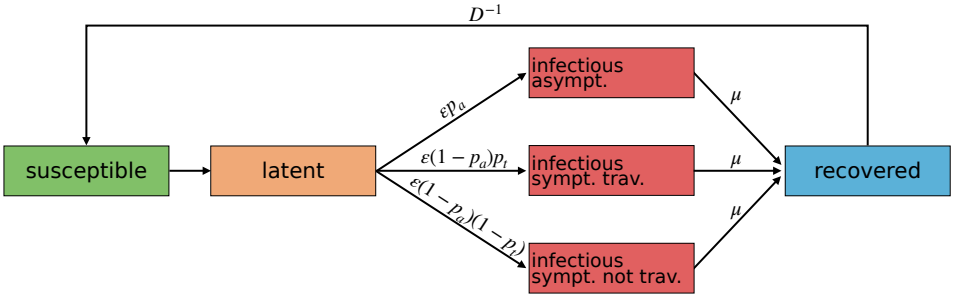


Figure S1: Scheme of the compartmental model. Expressions for the transition probabilities are reported in Tab. S2.

Table S1: Transitions between compartments and their rates.

| Transition | Type | Rate |
|---|---|---|
| $S_j \to L_j$ | Contagion | $\lambda_j$ |
| $L_j \to I_j^a$ | Spontaneous | $\varepsilon p_a$ |
| $L_j \to I_j^t$ | ” | $\varepsilon(1-p_a)p_t$ |
| $L_j \to I_j^{nt}$ | ” | $\varepsilon(1-p_a)(1-p_t)$ |
| $I_j^a \to R_j$ | ” | $\mu$ |
| $I_j^t \to R_j$ | ” | $\mu$ |
| $I_j^{nt} \to R_j$ | ” | $\mu$ |
| $R_j \to S_j$ | ” | $D^{-1}$ |

symptoms, and Recovered. The rate at which a susceptible individual in patch $j$ acquires the infection, the so-called force of infection $\lambda_j$, is determined by interactions with infectious persons either in the home patch $j$ or in its neighboring patches on the commuting network. Individuals mix homogeneously with other individuals sharing the same home patch $j$. The level of mixing with individuals in neighboring patches is instead modulated by commuting probability and duration, as detailed in [3, 4]. Overall transmission is modulated by the parameter $\beta_i$, representing the intrinsic viral transmissibility that depends on the patch $i$ where mixing occurs.

Given the force of infection $\lambda_j$ in patch $j$, each person in the susceptible compartment $(S_j)$ contracts the infection with probability $\lambda_j \Delta t$ and enters the latent compartment $(L_j)$, where $\Delta t$ is the time interval considered. Latent individuals exit the compartment with probability $\varepsilon \Delta t$, and transit to

Table S2: Summary of parameters and their values

| Parameter | Value |
|---|---|
| $\beta(t)$ | computed from Eq.( 4) |
| $\mu$ | 1/2.5 days [11] |
| $\epsilon$ | 1/1.1 days [11] |
| $p_a$ | 0.33 [12] |
| $p_t$ | 0.5 [12] |
| $r_\beta$ | 0.5 [12] |
| $D$ | explored |
| $R_{\min}$ | explored |
| $R_{\max}$ | explored |
| $t_{\max}$ | explored |

asymptomatic infectious compartment ($I_j^a$) with probability $p_a$ or, with the complementary probability $1 - p_a$, become symptomatic infectious. Infectious persons with symptoms are further divided between those who can travel ($I_j^t$), probability $p_t$, and those who are travel-restricted due to severe symptoms ($I_j^{nt}$) with probability $1 - p_t$. Asymptomatic individuals are assumed to have infection potential reduced by a factor $r_\beta$ with respect to individuals showing symptoms. All the infectious persons fully recover with probability $\mu\Delta t$, entering the recovered compartment ($R_j$) in the next time step. Recovered individuals lose their immunity and become fully susceptible again with rate $D^{-1}$. A schematic representation of the compartmental model is reported in Fig. S1, all transitions and corresponding rates are summarized in Table S1, while parameter values are reported in Table S2.

For the compartmental model above described the basic reproduction number ($R_0$) is given by

$$R_0 = \beta\mu^{-1}[1 - p_a + r_\beta p_a]. \tag{4}$$

### 1.4 Seasonality in transmission

In order to model the seasonality effect in the northern and in the southern hemispheres, we follow the approach of Cooper et al. [13] rescaling the basic reproduction ratio $R_0$ by a sinusoidal function,

$$R_{0,h}(t) = \frac{R_{\max}}{2}\left[\left(1 - \frac{R_{\min}}{R_{\max}}\right)\sin\left(\frac{2\pi}{365}(t - t_{max,\,h}) + \frac{\pi}{2}\right) + 1 + \frac{R_{\min}}{R_{\max}}\right],$$

where $h$ refers to the seasonal area (among northern hemisphere, southern hemisphere, tropics) each patch belongs to. In the tropical region, $R_0$ is identically equal to $R_{\max}$. $t_{\max,\,h}$ is the time corresponding to the maximum of the sinusoid and hence to the maximum of the effective $R_0$, $R_{\max}$. The time of maximum transmissibility in the southern hemisphere, $t_{\max,\,s}$ occurs six months out of phase with respect to the northern hemisphere ($t_{\max,\,n}$). The parameters $t_{\max,\,n}$, $R_{\min}$ and $R_{\max}$ were calibrated as detailed in the following section. Tab. S2 summarizes all parameters and their values.

### 1.5 Stochastic simulations

For each set of parameters and for each version of the model, we run stochastic simulations of 28-year global circulation of influenza. Simulations are in discrete time with a temporal resolution of one day. At each time step, multinomial extractions associated with traveling and infection dynamics rules are performed for each patch. To ensure that the dynamics converge to an active epidemic state, we started with an initial configuration roughly close to the equilibrium configuration. In particular, we assumed for each patch a non negligible fraction of the population to be symptomatic infectious (0.0001), a fraction $1-1/R_{\max}$ to be recovered, and the rest susceptible. Alternative initial conditions were tested and showed that different occupation numbers of the compartments and different distributions of infectious across patches (i.e. a single infected patch instead of all patches) were affecting the probability of observing epidemic extinction at the beginning and the intensity of the epidemic peaks during the transient stage, while, instead, the average incidence and the number of imported cases computed across years and runs, after discarding the initial epidemic period, were robust to initial conditions. The initial transient-dynamics period discarded was 8 years. We run 36 stochastic simulations for each scenario. After preliminary tests, this number was found to be sufficient to properly reconstruct the space of dynamic trajectories.

Daily traveling infectious cases from one city to another simulated with GLEAM are spatially aggregated at the country level by summing the fluxes between airports situated within the same pair of countries. These fluxes are then aggregated in time by summing them over specified time intervals, either annually or within six-month periods - from March 21 to September 20 and from September 21 to March 20, named throughout the text April-September and October-March, respectively. We obtained, in this way, the matrices containing the annual and seasonal influenza migration fluxes.

Different $R_{\max}$, $R_{\min}$, $t_{\max}$ and $D$ were compared. Specifically, values

tested where: $R_{\max} \in [1.25, 1.5, 1.75, 2.0, 2.25, 2.5]$ [14]; $R_{\min} \in [0.5, 0.75]$ (exploring different levels of subcritical transmission [15]);
$t_{\max} \in [\text{Nov 15th}, \text{Dec 15th}, \text{Jan 15th}]$ and $D \in [1, 2, 4, 6, 8]$ [16, 17, 18, 19].

## 2 Phylogeographic GLM analysis

We employ a generalized linear model (GLM) formulation of a continuous-time Markov chain (CTMC) process[20] to test how simulated fluxes predict phylogeographic diffusion. This model parameterizes the instantaneous movement rate $\Lambda_{ij}$ from location $i$ to location $j$ as a log-linear function of $P$ potential predictors $\mathbf{X}_{ij} = (x_{ij1}, \ldots, x_{ijP})^{'}$ with unknown coefficients $\boldsymbol{\beta} = (\beta_1, \ldots, \beta_P)^{'}$ and diagonal matrix $\boldsymbol{\delta}$ with entries $(\delta_1, \ldots, \delta_P)$. These latter unknown indicators $\delta_p \in \{0, 1\}$ determine predictor $p$'s inclusion in or exclusion from the model. We refer to [20] for the details of drawing posterior inference under the standard GLM-diffusion model. Because we aim to compare the support for individual model-based fluxes out of $P$ possible fluxes, instead of allowing all possible combinations of different predictors as in previous applications, we replace the standard transition kernel on the indicator variables that determine predictor inclusion by a new transition kernel that proposes a single randomly chosen predictor to replace the current predictor in the GLM model. The inclusion of only a single predictor removes the need to specify a prior probability over the inclusion probabilities that prefer a sparse set of predictors a priori. Instead, each flux has a prior probability of $1/P$ to be included in the model. We follow [20] in specifying that a priori all $\beta_p$ are independent and normally distributed with mean 0 and a relatively large variance of 4.

To consider time-inhomogeneity in the spatial diffusion process, we borrow epoch modeling concepts from [21]. The epoch GLM parameterizes the instantaneous movement rate $\Lambda_{ijt}$ from state $i$ to state $j$ within epoch $t$ as a log-linear function of $P$ epoch-specific predictors $\mathbf{X}_{ijt} = (x_{ijt1}, \ldots, x_{ijtP})^{'}$ with constant-through-time, unknown coefficients $\boldsymbol{\beta}$. As epoch-specific predictors, we use the aggregated GLEAM fluxes from two consecutive six-month periods. These fluxes are considered predictors for their corresponding alternating periods throughout the evolutionary history. We report posterior expectations for the inclusion probabilities associated with each flux.

Using the time-inhomogeneous (epoch) GLM-diffusion approach, we compare fluxes based on the standard air-passenger network with Markovian and the recurrent travel version of GLEAM (Supplementary Table S3), either as seasonally aggregated fluxes over time against annually aggregated fluxes

(Supplementary Table S4), as well as peak time represented by January against December (Supplementary Table S5) and November against December (Supplementary Table S6) for the full H3N2 (H3), H1N1(H1), Yamagata (YAM) and Victoria (VIC) data sets. These Supplementary Tables are also available at `https://github.com/phylogeography/GLEAM-phylogeography` We use BEAST [22] to estimate posterior distributions for the parameters in the various phylogeographic models in conjunction with the BEAGLE library [23] to speed up likelihood calculations.

## 3 Simulation study

We evaluate the performance of the phylogeographic GLM procedure by simulating discrete diffusion processes for five different predictors. Specifically, 20 replicates of discrete diffusion processes were simulated using $\pi$BUSS [24] according to air travel and four different time-homogeneous GLEAM flux predictors. The posterior inclusion probabilities averaged over the 20 replicates demonstrate that we are generally able to find good support for the predictor that was used to simulate the discrete diffusion process (Fig. S2). Specifically, we generally recover good support for air travel fluxes for diffusion processes simulated according to this predictor (Fig. S2A). We also consistently recover the highest support for the specific GLEAM parameter values that were used in the simulations with GLEAM flux predictors (Fig. S2B-E), even though they can be associated with considerable uncertainty. However, in cases with uncertainty (e.g. D inclusion probabilities in Fig. S2B and Fig. S2E or Rmax inclusion probabilities in Fig. S2D and Fig. S2E), only values close to the true parameters receive substantial support. Finally, we find overwhelming support for time-homogeneous fluxes (annual), as used in the simulations, as opposed to time-inhomogeneous fluxes (seasonal).

Table S3: Inclusion probabilities for the phylogeographic GLM comparison (C) of fluxes based on both Markovian (M) and recurrent travel (i.e. non-Markovian, NM) GLEAM parameterizations. The highest inclusion probabilities for each data set are shown in bold, non-zero rates in italic and zero values are represented by hyphens.

| $R_{max}$ | $R_{min}$ | D | C | $H3_{nr}$ | $H3_{r}$ | $H1_{nr}$ | $H1_{r}$ | $YAM_{nr}$ | $YAM_{r}$ | $VIC_{nr}$ | $VIC_{r}$ |
|---|---|---|---|---|---|---|---|---|---|---|---|
| (air) | (air) | (air) | (air) | - | - | - | *0.02* | - | - | - | **0.95** |
| 1.25 | 0.5 | 1 | M | - | - | - | - | - | - | - | - |
| 1.25 | 0.5 | 2 | M | - | - | - | - | - | - | - | - |
| 1.25 | 0.5 | 4 | M | - | - | - | - | - | - | - | - |
| 1.25 | 0.5 | 6 | M | - | - | - | - | - | - | - | - |
| 1.25 | 0.5 | 8 | M | - | - | - | - | - | - | - | - |
| 1.25 | 0.75 | 1 | M | - | - | - | - | - | - | - | - |
| 1.25 | 0.75 | 2 | M | - | - | - | - | - | - | - | - |
| 1.25 | 0.75 | 4 | M | - | - | - | - | - | - | - | - |
| 1.25 | 0.75 | 6 | M | - | - | - | - | - | - | - | - |
| 1.25 | 0.75 | 8 | M | - | - | - | - | - | - | - | - |
| 1.5 | 0.5 | 1 | M | - | - | - | - | - | - | - | - |
| 1.5 | 0.5 | 2 | M | - | - | - | - | - | - | - | - |
| 1.5 | 0.5 | 4 | M | - | - | - | - | - | - | - | - |
| 1.5 | 0.5 | 6 | M | - | - | - | - | - | - | - | - |
| 1.5 | 0.5 | 8 | M | - | - | - | - | - | - | - | - |
| 1.5 | 0.75 | 1 | M | - | - | - | - | - | - | - | - |
| 1.5 | 0.75 | 2 | M | - | - | - | - | - | - | - | - |
| 1.5 | 0.75 | 4 | M | - | - | - | - | - | - | - | - |
| 1.5 | 0.75 | 6 | M | - | - | - | - | - | - | - | - |
| 1.5 | 0.75 | 8 | M | - | - | - | - | - | - | - | - |
| 1.75 | 0.5 | 1 | M | - | - | - | - | - | - | - | - |
| 1.75 | 0.5 | 2 | M | - | - | - | - | - | - | - | - |
| 1.75 | 0.5 | 4 | M | - | - | - | - | - | - | - | - |
| 1.75 | 0.5 | 6 | M | - | - | - | - | - | - | - | - |
| 1.75 | 0.5 | 8 | M | - | - | - | - | - | - | - | - |
| 1.75 | 0.75 | 1 | M | - | - | - | - | - | - | - | - |
| 1.75 | 0.75 | 2 | M | - | - | - | - | - | - | - | - |
| 1.75 | 0.75 | 4 | M | - | - | - | - | - | - | - | - |
| 1.75 | 0.75 | 6 | M | - | - | - | - | - | - | - | - |
| 1.75 | 0.75 | 8 | M | - | - | - | - | - | - | - | - |
| 2 | 0.5 | 1 | M | - | - | - | - | - | - | - | - |
| 2 | 0.5 | 2 | M | - | - | - | - | - | - | - | - |
| 2 | 0.5 | 4 | M | - | - | - | - | - | - | - | - |

| | | | | | | | | | | | |
|---|---|---|---|---|---|---|---|---|---|---|---|
| 2 | 0.5 | 6 | M | - | - | - | - | - | - | - | - |
| 2 | 0.5 | 8 | M | - | - | - | - | - | - | - | - |
| 2 | 0.75 | 1 | M | - | - | - | - | - | - | - | - |
| 2 | 0.75 | 2 | M | - | - | - | - | - | - | - | - |
| 2 | 0.75 | 4 | M | - | - | - | - | - | - | - | - |
| 2 | 0.75 | 6 | M | - | - | - | - | - | - | - | - |
| 2 | 0.75 | 8 | M | - | - | - | - | - | - | - | - |
| 2.25 | 0.5 | 1 | M | - | - | - | - | - | - | - | - |
| 2.25 | 0.5 | 2 | M | - | - | - | - | - | - | - | - |
| 2.25 | 0.5 | 4 | M | - | - | - | - | - | - | - | - |
| 2.25 | 0.5 | 6 | M | - | - | - | - | - | - | - | - |
| 2.25 | 0.5 | 8 | M | - | - | - | - | - | - | - | - |
| 2.25 | 0.75 | 1 | M | - | - | - | - | - | - | - | - |
| 2.25 | 0.75 | 2 | M | - | - | - | - | - | - | - | - |
| 2.25 | 0.75 | 4 | M | - | - | - | - | - | - | - | - |
| 2.25 | 0.75 | 6 | M | - | - | - | - | - | - | - | - |
| 2.25 | 0.75 | 8 | M | - | - | - | - | - | - | - | - |
| 2.5 | 0.5 | 1 | M | - | - | - | - | - | - | - | - |
| 2.5 | 0.5 | 2 | M | - | - | - | - | - | - | - | - |
| 2.5 | 0.5 | 4 | M | - | - | - | - | - | - | - | - |
| 2.5 | 0.5 | 6 | M | - | - | - | - | - | - | - | - |
| 2.5 | 0.5 | 8 | M | - | - | - | - | - | - | - | - |
| 2.5 | 0.75 | 1 | M | - | - | - | - | - | - | - | - |
| 2.5 | 0.75 | 2 | M | - | - | - | - | - | - | - | - |
| 2.5 | 0.75 | 4 | M | - | - | - | - | - | - | - | - |
| 2.5 | 0.75 | 6 | M | - | - | - | - | - | - | - | - |
| 2.5 | 0.75 | 8 | M | - | - | - | - | - | - | - | - |
| 1.25 | 0.5 | 1 | NM | - | - | - | - | - | - | - | - |
| 1.25 | 0.5 | 2 | NM | - | - | - | - | - | - | - | - |
| 1.25 | 0.5 | 4 | NM | - | - | - | - | - | - | - | - |
| 1.25 | 0.5 | 6 | NM | - | - | - | - | - | - | - | - |
| 1.25 | 0.5 | 8 | NM | - | - | - | - | - | - | - | - |
| 1.25 | 0.75 | 1 | NM | - | - | - | - | - | - | - | - |
| 1.25 | 0.75 | 2 | NM | - | - | - | - | - | - | - | - |
| 1.25 | 0.75 | 4 | NM | - | - | - | - | - | - | - | - |
| 1.25 | 0.75 | 6 | NM | - | - | - | - | - | - | - | - |
| 1.25 | 0.75 | 8 | NM | - | - | - | - | - | - | - | - |
| 1.5 | 0.5 | 1 | NM | - | - | *0.19* | *0.02* | - | - | - | - |
| 1.5 | 0.5 | 2 | NM | - | - | 0.01 | - | - | - | - | - |
| 1.5 | 0.5 | 4 | NM | - | - | - | - | - | - | - | - |

| | | | | | | | | | | | |
|---|---|---|---|---|---|---|---|---|---|---|---|
| 1.5 | 0.5 | 6 | NM | - | - | - | - | - | - | - | - |
| 1.5 | 0.5 | 8 | NM | - | - | - | - | - | - | - | - |
| 1.5 | 0.75 | 1 | NM | - | - | **0.32** | *0.15* | - | *0.01* | *0.01* | - |
| 1.5 | 0.75 | 2 | NM | - | - | *0.01* | - | - | - | - | - |
| 1.5 | 0.75 | 4 | NM | - | - | - | - | - | - | - | - |
| 1.5 | 0.75 | 6 | NM | - | - | - | - | - | - | - | - |
| 1.5 | 0.75 | 8 | NM | - | - | - | - | - | - | - | - |
| 1.75 | 0.5 | 1 | NM | - | - | - | - | - | *0.01* | - | - |
| 1.75 | 0.5 | 2 | NM | - | - | *0.01* | *0.01* | *0.01* | *0.02* | *0.04* | - |
| 1.75 | 0.5 | 4 | NM | - | - | *0.01* | - | - | - | - | - |
| 1.75 | 0.5 | 6 | NM | - | - | - | - | - | - | - | - |
| 1.75 | 0.5 | 8 | NM | - | - | - | - | - | - | - | - |
| 1.75 | 0.75 | 1 | NM | - | - | - | *0.01* | - | *0.01* | - | - |
| 1.75 | 0.75 | 2 | NM | - | - | *0.03* | *0.02* | *0.08* | *0.09* | - | - |
| 1.75 | 0.75 | 4 | NM | - | - | - | - | - | - | - | - |
| 1.75 | 0.75 | 6 | NM | - | - | - | - | - | - | - | - |
| 1.75 | 0.75 | 8 | NM | - | - | - | - | - | - | - | - |
| 2 | 0.5 | 1 | NM | - | - | - | - | - | - | - | - |
| 2 | 0.5 | 2 | NM | - | - | - | - | *0.03* | *0.09* | *0.05* | - |
| 2 | 0.5 | 4 | NM | - | - | *0.01* | *0.01* | - | - | - | - |
| 2 | 0.5 | 6 | NM | - | - | - | *0.01* | - | - | - | - |
| 2 | 0.5 | 8 | NM | - | - | - | - | - | - | - | - |
| 2 | 0.75 | 1 | NM | - | - | - | - | - | - | - | - |
| 2 | 0.75 | 2 | NM | - | - | *0.03* | *0.02* | **0.73** | **0.46** | **0.77** | - |
| 2 | 0.75 | 4 | NM | - | - | - | *0.02* | - | *0.01* | - | - |
| 2 | 0.75 | 6 | NM | - | - | - | - | - | - | - | - |
| 2 | 0.75 | 8 | NM | - | - | - | - | - | - | - | - |
| 2.25 | 0.5 | 1 | NM | - | - | - | - | - | - | - | - |
| 2.25 | 0.5 | 2 | NM | **0.32** | - | *0.03* | *0.04* | *0.01* | *0.08* | *0.03* | - |
| 2.25 | 0.5 | 4 | NM | - | - | - | *0.02* | - | *0.02* | - | - |
| 2.25 | 0.5 | 6 | NM | - | - | - | *0.01* | - | - | - | - |
| 2.25 | 0.5 | 8 | NM | - | - | - | - | - | - | - | - |
| 2.25 | 0.75 | 1 | NM | - | - | - | - | - | - | - | - |
| 2.25 | 0.75 | 2 | NM | **0.68** | **1.00** | **0.30** | **0.51** | - | - | *0.06* | - |
| 2.25 | 0.75 | 4 | NM | - | - | - | *0.01* | - | *0.02* | *0.01* | - |
| 2.25 | 0.75 | 6 | NM | - | - | - | *0.01* | - | - | - | - |
| 2.25 | 0.75 | 8 | NM | - | - | - | - | - | - | - | - |
| 2.5 | 0.5 | 1 | NM | - | - | - | - | - | - | - | - |
| 2.5 | 0.5 | 2 | NM | - | - | - | *0.01* | - | *0.01* | - | - |
| 2.5 | 0.5 | 4 | NM | - | - | - | - | *0.03* | *0.04* | *0.01* | - |

| | | | | | | | | | | | |
|---|---|---|---|---|---|---|---|---|---|---|---|
| 2.5 | 0.5 | 6 | NM | - | - | - | *0.02* | - | - | - | - |
| 2.5 | 0.5 | 8 | NM | - | - | - | - | - | - | - | - |
| 2.5 | 0.75 | 1 | NM | - | - | - | - | - | - | - | - |
| 2.5 | 0.75 | 2 | NM | - | - | - | *0.01* | - | *0.02* | - | - |
| 2.5 | 0.75 | 4 | NM | - | - | - | - | *0.09* | *0.07* | *0.02* | - |
| 2.5 | 0.75 | 6 | NM | - | - | - | *0.03* | - | *0.01* | - | - |
| 2.5 | 0.75 | 8 | NM | - | - | - | *0.01* | - | - | - | - |

Table S4: Inclusion probabilities for the phylogeographic GLM comparison (C) of annually-aggregated (A) and seasonally-aggregated (S) fluxes based on different in a non-Markovian GLEAM parameterizations. The highest inclusion probabilities for each data set are shown in bold, non-zero rates in italic and zero values are represented by hyphens.

| $R_{max}$ | $R_{min}$ | D | C | $H3_{nr}$ | $H3_{r}$ | $H1_{nr}$ | $H1_{r}$ | $YAM_{nr}$ | $YAM_{r}$ | $VIC_{nr}$ | $VIC_{r}$ |
|---|---|---|---|---|---|---|---|---|---|---|---|
| (air) | (air) | (air) | (air) | - | - | - | *0.02* | - | - | - | **0.95** |
| 1.25 | 0.5 | 1 | A | - | - | - | - | - | - | - | - |
| 1.25 | 0.5 | 2 | A | - | - | - | - | - | - | - | - |
| 1.25 | 0.5 | 4 | A | - | - | - | - | - | - | - | - |
| 1.25 | 0.5 | 6 | A | - | - | - | - | - | - | - | - |
| 1.25 | 0.5 | 8 | A | - | - | - | - | - | - | - | - |
| 1.25 | 0.75 | 1 | A | - | - | - | - | - | - | - | - |
| 1.25 | 0.75 | 2 | A | - | - | - | - | - | - | - | - |
| 1.25 | 0.75 | 4 | A | - | - | - | - | - | - | - | - |
| 1.25 | 0.75 | 6 | A | - | - | - | - | - | - | - | - |
| 1.25 | 0.75 | 8 | A | - | - | - | - | - | - | - | - |
| 1.5 | 0.5 | 1 | A | - | - | - | - | - | - | - | - |
| 1.5 | 0.5 | 2 | A | - | - | - | - | - | - | - | - |
| 1.5 | 0.5 | 4 | A | - | - | - | - | - | - | - | - |
| 1.5 | 0.5 | 6 | A | - | - | - | - | - | - | - | - |
| 1.5 | 0.5 | 8 | A | - | - | - | - | - | - | - | - |
| 1.5 | 0.75 | 1 | A | - | - | - | - | - | - | - | - |
| 1.5 | 0.75 | 2 | A | - | - | - | - | - | - | - | - |
| 1.5 | 0.75 | 4 | A | - | - | - | - | - | - | - | - |
| 1.5 | 0.75 | 6 | A | - | - | - | - | - | - | - | - |
| 1.5 | 0.75 | 8 | A | - | - | - | - | - | - | - | - |
| 1.75 | 0.5 | 1 | A | - | - | - | - | - | - | - | - |
| 1.75 | 0.5 | 2 | A | - | - | - | - | - | - | - | - |
| 1.75 | 0.5 | 4 | A | - | - | - | - | - | - | - | - |
| 1.75 | 0.5 | 6 | A | - | - | - | - | - | - | - | - |

| | | | | | | | | | | | |
|---|---|---|---|---|---|---|---|---|---|---|---|
| 1.75 | 0.5 | 8 | A | - | - | - | - | - | - | - | - |
| 1.75 | 0.75 | 1 | A | - | - | - | - | - | - | - | - |
| 1.75 | 0.75 | 2 | A | - | - | - | - | - | - | - | - |
| 1.75 | 0.75 | 4 | A | - | - | - | - | - | - | - | - |
| 1.75 | 0.75 | 6 | A | - | - | - | - | - | - | - | - |
| 1.75 | 0.75 | 8 | A | - | - | - | - | - | - | - | - |
| 2 | 0.5 | 1 | A | - | - | - | - | - | - | - | - |
| 2 | 0.5 | 2 | A | - | - | - | - | - | - | - | - |
| 2 | 0.5 | 4 | A | - | - | - | - | - | - | - | - |
| 2 | 0.5 | 6 | A | - | - | - | - | - | - | - | - |
| 2 | 0.5 | 8 | A | - | - | - | - | - | - | - | - |
| 2 | 0.75 | 1 | A | - | - | - | - | - | - | - | - |
| 2 | 0.75 | 2 | A | - | - | - | - | - | - | - | - |
| 2 | 0.75 | 4 | A | - | - | - | - | - | - | - | - |
| 2 | 0.75 | 6 | A | - | - | - | - | - | - | - | - |
| 2 | 0.75 | 8 | A | - | - | - | - | - | - | - | - |
| 2.25 | 0.5 | 1 | A | - | - | - | - | - | - | - | - |
| 2.25 | 0.5 | 2 | A | - | - | - | - | - | - | - | - |
| 2.25 | 0.5 | 4 | A | - | - | - | - | - | - | - | - |
| 2.25 | 0.5 | 6 | A | - | - | - | - | - | - | - | - |
| 2.25 | 0.5 | 8 | A | - | - | - | - | - | - | - | - |
| 2.25 | 0.75 | 1 | A | - | - | - | - | - | - | - | - |
| 2.25 | 0.75 | 2 | A | - | - | - | - | - | - | - | - |
| 2.25 | 0.75 | 4 | A | - | - | - | - | - | - | - | - |
| 2.25 | 0.75 | 6 | A | - | - | - | - | - | - | - | - |
| 2.25 | 0.75 | 8 | A | - | - | - | - | - | - | - | - |
| 2.5 | 0.5 | 1 | A | - | - | - | - | - | - | - | - |
| 2.5 | 0.5 | 2 | A | - | - | - | - | - | - | - | - |
| 2.5 | 0.5 | 4 | A | - | - | - | - | - | - | - | - |
| 2.5 | 0.5 | 6 | A | - | - | - | - | - | - | - | - |
| 2.5 | 0.5 | 8 | A | - | - | - | - | - | - | - | - |
| 2.5 | 0.75 | 1 | A | - | - | - | - | - | - | - | - |
| 2.5 | 0.75 | 2 | A | - | - | - | - | - | - | - | - |
| 2.5 | 0.75 | 4 | A | - | - | - | - | - | - | - | - |
| 2.5 | 0.75 | 6 | A | - | - | - | - | - | - | - | - |
| 2.5 | 0.75 | 8 | A | - | - | - | - | - | - | - | - |
| 1.25 | 0.5 | 1 | S | - | - | - | - | - | - | - | - |
| 1.25 | 0.5 | 2 | S | - | - | - | - | - | - | - | - |
| 1.25 | 0.5 | 4 | S | - | - | - | - | - | - | - | - |
| 1.25 | 0.5 | 6 | S | - | - | - | - | - | - | - | - |

| | | | | | | | | | | | |
|---|---|---|---|---|---|---|---|---|---|---|---|
| 1.25 | 0.5 | 8 | S | - | - | - | - | - | - | - | - |
| 1.25 | 0.75 | 1 | S | - | - | - | - | - | - | - | - |
| 1.25 | 0.75 | 2 | S | - | - | - | - | - | - | - | - |
| 1.25 | 0.75 | 4 | S | - | - | - | - | - | - | - | - |
| 1.25 | 0.75 | 6 | S | - | - | - | - | - | - | - | - |
| 1.25 | 0.75 | 8 | S | - | - | - | - | - | - | - | - |
| 1.5 | 0.5 | 1 | S | - | - | *0.20* | *0.02* | - | - | - | - |
| 1.5 | 0.5 | 2 | S | - | - | *0.01* | - | - | - | - | - |
| 1.5 | 0.5 | 4 | S | - | - | - | - | - | - | - | - |
| 1.5 | 0.5 | 6 | S | - | - | - | - | - | - | - | - |
| 1.5 | 0.5 | 8 | S | - | - | - | - | - | - | - | - |
| 1.5 | 0.75 | 1 | S | - | - | **0.32** | *0.15* | - | *0.01* | *0.01* | - |
| 1.5 | 0.75 | 2 | S | - | - | *0.01* | - | - | - | - | - |
| 1.5 | 0.75 | 4 | S | - | - | - | - | - | - | - | - |
| 1.5 | 0.75 | 6 | S | - | - | - | - | - | - | - | - |
| 1.5 | 0.75 | 8 | S | - | - | - | - | - | - | - | - |
| 1.75 | 0.5 | 1 | S | - | - | - | - | - | *0.01* | - | - |
| 1.75 | 0.5 | 2 | S | - | - | *0.01* | *0.01* | *0.01* | *0.02* | *0.04* | - |
| 1.75 | 0.5 | 4 | S | - | - | *0.01* | - | - | - | - | - |
| 1.75 | 0.5 | 6 | S | - | - | - | - | - | - | - | - |
| 1.75 | 0.5 | 8 | S | - | - | - | - | - | - | - | - |
| 1.75 | 0.75 | 1 | S | - | - | - | *0.01* | - | *0.01* | - | - |
| 1.75 | 0.75 | 2 | S | - | - | *0.03* | *0.02* | *0.09* | *0.09* | - | - |
| 1.75 | 0.75 | 4 | S | - | - | - | - | - | - | - | - |
| 1.75 | 0.75 | 6 | S | - | - | - | - | - | - | - | - |
| 1.75 | 0.75 | 8 | S | - | - | - | - | - | - | - | - |
| 2 | 0.5 | 1 | S | - | - | - | - | - | - | - | - |
| 2 | 0.5 | 2 | S | - | - | - | - | *0.03* | *0.09* | *0.06* | - |
| 2 | 0.5 | 4 | S | - | - | *0.01* | *0.01* | - | - | - | - |
| 2 | 0.5 | 6 | S | - | - | *0.01* | *0.01* | - | - | - | - |
| 2 | 0.5 | 8 | S | - | - | - | - | - | - | - | - |
| 2 | 0.75 | 1 | S | - | - | - | - | - | - | - | - |
| 2 | 0.75 | 2 | S | - | - | *0.03* | *0.02* | **0.73** | **0.46** | **0.77** | - |
| 2 | 0.75 | 4 | S | - | - | - | *0.02* | - | *0.01* | - | - |
| 2 | 0.75 | 6 | S | - | - | - | - | - | - | - | - |
| 2 | 0.75 | 8 | S | - | - | - | - | - | - | - | - |
| 2.25 | 0.5 | 1 | S | - | - | - | - | - | - | - | - |
| 2.25 | 0.5 | 2 | S | **0.32** | - | *0.03* | *0.04* | *0.01* | *0.07* | *0.03* | - |
| 2.25 | 0.5 | 4 | S | - | - | - | *0.02* | - | *0.02* | - | - |
| 2.25 | 0.5 | 6 | S | - | - | - | *0.01* | - | - | - | - |

| | | | | | | | | | | | |
|---|---|---|---|---|---|---|---|---|---|---|---|
| 2.25 | 0.5 | 8 | S | - | - | - | - | - | - | - | - |
| 2.25 | 0.75 | 1 | S | - | - | - | - | - | - | - | - |
| 2.25 | 0.75 | 2 | S | **0.68** | **0.99** | **0.29** | **0.48** | - | - | *0.06* | - |
| 2.25 | 0.75 | 4 | S | - | - | - | *0.02* | - | *0.02* | *0.01* | - |
| 2.25 | 0.75 | 6 | S | - | - | - | *0.02* | - | - | - | - |
| 2.25 | 0.75 | 8 | S | - | - | - | - | - | - | - | - |
| 2.5 | 0.5 | 1 | S | - | - | - | - | - | - | - | - |
| 2.5 | 0.5 | 2 | S | - | - | - | *0.01* | - | *0.01* | - | - |
| 2.5 | 0.5 | 4 | S | - | - | - | - | *0.03* | *0.04* | *0.01* | - |
| 2.5 | 0.5 | 6 | S | - | - | *0.01* | *0.02* | - | - | - | - |
| 2.5 | 0.5 | 8 | S | - | - | - | - | - | - | - | - |
| 2.5 | 0.75 | 1 | S | - | - | - | - | - | - | - | - |
| 2.5 | 0.75 | 2 | S | - | - | - | *0.01* | - | *0.01* | - | - |
| 2.5 | 0.75 | 4 | S | - | - | - | - | *0.09* | *0.08* | *0.02* | - |
| 2.5 | 0.75 | 6 | S | - | - | - | *0.02* | - | *0.01* | - | - |
| 2.5 | 0.75 | 8 | S | - | - | - | *0.01* | - | - | - | - |

Table S5: Inclusion probabilities for the phylogeographic GLM comparison (C) of peak time between December-aggregated (Dec) and January-aggregated (Jan) fluxes based on a non-Markovian GLEAM parameterization. The highest inclusion probabilities for each data set are shown in bold, non-zero rates in italic and zero values are represented by hyphens.

| $R_{max}$ | $R_{min}$ | D | C | $H3_{nr}$ | $H3_{r}$ | $H1_{nr}$ | $H1_{r}$ | $YAM_{nr}$ | $YAM_{r}$ | $VIC_{nr}$ | $VIC_{r}$ |
|---|---|---|---|---|---|---|---|---|---|---|---|
| (air) | (air) | (air) | (air) | - | - | - | *0.02* | - | - | - | **0.96** |
| 1.25 | 0.5 | 1 | Dec | - | - | - | - | - | - | - | - |
| 1.25 | 0.5 | 2 | Dec | - | - | - | - | - | - | - | - |
| 1.25 | 0.5 | 4 | Dec | - | - | - | - | - | - | - | - |
| 1.25 | 0.5 | 6 | Dec | - | - | - | - | - | - | - | - |
| 1.25 | 0.5 | 8 | Dec | - | - | - | - | - | - | - | - |
| 1.25 | 0.75 | 1 | Dec | - | - | - | - | - | - | - | - |
| 1.25 | 0.75 | 2 | Dec | - | - | - | - | - | - | - | - |
| 1.25 | 0.75 | 4 | Dec | - | - | - | - | - | - | - | - |
| 1.25 | 0.75 | 6 | Dec | - | - | - | - | - | - | - | - |
| 1.25 | 0.75 | 8 | Dec | - | - | - | - | - | - | - | - |
| 1.5 | 0.5 | 1 | Dec | - | - | - | - | - | - | - | - |
| 1.5 | 0.5 | 2 | Dec | - | - | - | - | - | - | - | - |
| 1.5 | 0.5 | 4 | Dec | - | - | - | - | - | - | - | - |
| 1.5 | 0.5 | 6 | Dec | - | - | - | - | - | - | - | - |

| | | | | | | | | | | | |
|---|---|---|---|---|---|---|---|---|---|---|---|
| 1.5 | 0.5 | 8 | Dec | - | - | - | - | - | - | - | - |
| 1.5 | 0.75 | 1 | Dec | - | - | - | - | - | - | - | - |
| 1.5 | 0.75 | 2 | Dec | - | - | - | - | - | - | - | - |
| 1.5 | 0.75 | 4 | Dec | - | - | - | - | - | - | - | - |
| 1.5 | 0.75 | 6 | Dec | - | - | - | - | - | - | - | - |
| 1.5 | 0.75 | 8 | Dec | - | - | - | - | - | - | - | - |
| 1.75 | 0.5 | 1 | Dec | - | - | - | - | - | - | - | - |
| 1.75 | 0.5 | 2 | Dec | - | - | - | - | - | - | - | - |
| 1.75 | 0.5 | 4 | Dec | - | - | - | - | - | - | - | - |
| 1.75 | 0.5 | 6 | Dec | - | - | - | - | - | - | - | - |
| 1.75 | 0.5 | 8 | Dec | - | - | - | - | - | - | - | - |
| 1.75 | 0.75 | 1 | Dec | - | - | - | - | - | - | - | - |
| 1.75 | 0.75 | 2 | Dec | - | - | - | - | - | - | - | - |
| 1.75 | 0.75 | 4 | Dec | - | - | - | - | - | - | - | - |
| 1.75 | 0.75 | 6 | Dec | - | - | - | - | - | - | - | - |
| 1.75 | 0.75 | 8 | Dec | - | - | - | - | - | - | - | - |
| 2 | 0.5 | 1 | Dec | - | - | - | - | - | - | - | - |
| 2 | 0.5 | 2 | Dec | - | - | - | - | - | - | - | - |
| 2 | 0.5 | 4 | Dec | - | - | - | - | - | - | - | - |
| 2 | 0.5 | 6 | Dec | - | - | - | - | - | - | - | - |
| 2 | 0.5 | 8 | Dec | - | - | - | - | - | - | - | - |
| 2 | 0.75 | 1 | Dec | - | - | - | - | - | - | - | - |
| 2 | 0.75 | 2 | Dec | - | - | - | - | - | - | - | - |
| 2 | 0.75 | 4 | Dec | - | - | - | - | - | - | - | - |
| 2 | 0.75 | 6 | Dec | - | - | - | - | - | - | - | - |
| 2 | 0.75 | 8 | Dec | - | - | - | - | - | - | - | - |
| 2.25 | 0.5 | 1 | Dec | - | - | - | - | - | - | - | - |
| 2.25 | 0.5 | 2 | Dec | - | - | - | - | - | - | - | - |
| 2.25 | 0.5 | 4 | Dec | - | - | - | - | - | - | - | - |
| 2.25 | 0.5 | 6 | Dec | - | - | - | - | - | - | - | - |
| 2.25 | 0.5 | 8 | Dec | - | - | - | - | - | - | - | - |
| 2.25 | 0.75 | 1 | Dec | - | - | - | - | - | - | - | - |
| 2.25 | 0.75 | 2 | Dec | - | - | - | - | - | - | - | - |
| 2.25 | 0.75 | 4 | Dec | - | - | - | - | - | - | - | - |
| 2.25 | 0.75 | 6 | Dec | - | - | - | - | - | - | - | - |
| 2.25 | 0.75 | 8 | Dec | - | - | - | - | - | - | - | - |
| 2.5 | 0.5 | 1 | Dec | - | - | - | - | - | - | - | - |
| 2.5 | 0.5 | 2 | Dec | - | - | - | - | - | - | - | - |
| 2.5 | 0.5 | 4 | Dec | - | - | - | - | - | - | - | - |
| 2.5 | 0.5 | 6 | Dec | - | - | - | - | - | - | - | - |

| | | | | | | | | | | | |
|---|---|---|---|---|---|---|---|---|---|---|---|
| 2.5 | 0.5 | 8 | Dec | - | - | - | - | - | - | - | - |
| 2.5 | 0.75 | 1 | Dec | - | - | - | - | - | - | - | - |
| 2.5 | 0.75 | 2 | Dec | - | - | - | - | - | - | - | - |
| 2.5 | 0.75 | 4 | Dec | - | - | - | - | - | - | - | - |
| 2.5 | 0.75 | 6 | Dec | - | - | - | - | - | - | - | - |
| 2.5 | 0.75 | 8 | Dec | - | - | - | - | - | - | - | - |
| 1.25 | 0.5 | 1 | Jan | - | - | - | - | - | - | - | - |
| 1.25 | 0.5 | 2 | Jan | - | - | - | - | - | - | - | - |
| 1.25 | 0.5 | 4 | Jan | - | - | - | - | - | - | - | - |
| 1.25 | 0.5 | 6 | Jan | - | - | - | - | - | - | - | - |
| 1.25 | 0.5 | 8 | Jan | - | - | - | - | - | - | - | - |
| 1.25 | 0.75 | 1 | Jan | - | - | - | - | - | - | - | - |
| 1.25 | 0.75 | 2 | Jan | - | - | - | - | - | - | - | - |
| 1.25 | 0.75 | 4 | Jan | - | - | - | - | - | - | - | - |
| 1.25 | 0.75 | 6 | Jan | - | - | - | - | - | - | - | - |
| 1.25 | 0.75 | 8 | Jan | - | - | - | - | - | - | - | - |
| 1.5 | 0.5 | 1 | Jan | - | - | *0.20* | *0.02* | - | - | - | - |
| 1.5 | 0.5 | 2 | Jan | - | - | *0.01* | - | - | - | - | - |
| 1.5 | 0.5 | 4 | Jan | - | - | - | - | - | - | - | - |
| 1.5 | 0.5 | 6 | Jan | - | - | - | - | - | - | - | - |
| 1.5 | 0.5 | 8 | Jan | - | - | - | - | - | - | - | - |
| 1.5 | 0.75 | 1 | Jan | - | - | **0.32** | *0.14* | - | *0.01* | *0.01* | *0.01* |
| 1.5 | 0.75 | 2 | Jan | - | - | *0.01* | - | - | - | - | - |
| 1.5 | 0.75 | 4 | Jan | - | - | - | - | - | - | - | - |
| 1.5 | 0.75 | 6 | Jan | - | - | - | - | - | - | - | - |
| 1.5 | 0.75 | 8 | Jan | - | - | - | - | - | - | - | - |
| 1.75 | 0.5 | 1 | Jan | - | - | - | - | - | - | - | - |
| 1.75 | 0.5 | 2 | Jan | - | - | *0.01* | *0.01* | *0.01* | *0.02* | *0.04* | - |
| 1.75 | 0.5 | 4 | Jan | - | - | *0.01* | - | - | - | - | - |
| 1.75 | 0.5 | 6 | Jan | - | - | - | - | - | - | - | - |
| 1.75 | 0.5 | 8 | Jan | - | - | - | - | - | - | - | - |
| 1.75 | 0.75 | 1 | Jan | - | - | - | *0.01* | - | *0.01* | - | - |
| 1.75 | 0.75 | 2 | Jan | - | - | *0.03* | *0.02* | *0.08* | *0.09* | - | - |
| 1.75 | 0.75 | 4 | Jan | - | - | - | - | - | - | - | - |
| 1.75 | 0.75 | 6 | Jan | - | - | - | - | - | - | - | - |
| 1.75 | 0.75 | 8 | Jan | - | - | - | - | - | - | - | - |
| 2 | 0.5 | 1 | Jan | - | - | - | - | - | - | - | - |
| 2 | 0.5 | 2 | Jan | - | - | - | - | *0.04* | *0.09* | *0.06* | - |
| 2 | 0.5 | 4 | Jan | - | - | *0.01* | *0.01* | - | - | - | - |
| 2 | 0.5 | 6 | Jan | - | - | - | *0.01* | - | - | - | - |

| | | | | | | | | | | | |
|---|---|---|---|---|---|---|---|---|---|---|---|
| 2 | 0.5 | 8 | Jan | - | - | - | - | - | - | - | - |
| 2 | 0.75 | 1 | Jan | - | - | - | - | - | - | - | - |
| 2 | 0.75 | 2 | Jan | - | - | *0.03* | *0.02* | **0.73** | **0.47** | **0.76** | - |
| 2 | 0.75 | 4 | Jan | - | - | - | *0.02* | - | *0.01* | - | - |
| 2 | 0.75 | 6 | Jan | - | - | - | - | - | - | - | - |
| 2 | 0.75 | 8 | Jan | - | - | - | - | - | - | - | - |
| 2.25 | 0.5 | 1 | Jan | - | - | - | - | - | - | - | - |
| 2.25 | 0.5 | 2 | Jan | **0.32** | - | *0.03* | *0.04* | *0.02* | *0.07* | *0.02* | - |
| 2.25 | 0.5 | 4 | Jan | - | - | - | *0.02* | - | *0.02* | - | - |
| 2.25 | 0.5 | 6 | Jan | - | - | - | *0.01* | - | - | - | - |
| 2.25 | 0.5 | 8 | Jan | - | - | - | - | - | - | - | - |
| 2.25 | 0.75 | 1 | Jan | - | - | - | - | - | - | - | - |
| 2.25 | 0.75 | 2 | Jan | **0.67** | **1.00** | **0.30** | **0.51** | - | - | *0.06* | *0.01* |
| 2.25 | 0.75 | 4 | Jan | - | - | - | *0.01* | - | *0.02* | *0.01* | - |
| 2.25 | 0.75 | 6 | Jan | - | - | - | *0.02* | - | - | - | - |
| 2.25 | 0.75 | 8 | Jan | - | - | - | - | - | - | - | - |
| 2.5 | 0.5 | 1 | Jan | - | - | - | - | - | - | - | - |
| 2.5 | 0.5 | 2 | Jan | - | - | - | *0.01* | - | *0.01* | - | - |
| 2.5 | 0.5 | 4 | Jan | - | - | - | - | *0.03* | *0.04* | *0.01* | - |
| 2.5 | 0.5 | 6 | Jan | - | - | *0.01* | *0.02* | - | - | - | - |
| 2.5 | 0.5 | 8 | Jan | - | - | - | - | - | - | - | - |
| 2.5 | 0.75 | 1 | Jan | - | - | - | - | - | - | - | - |
| 2.5 | 0.75 | 2 | Jan | - | - | - | *0.01* | - | *0.02* | - | - |
| 2.5 | 0.75 | 4 | Jan | - | - | - | - | *0.09* | *0.07* | *0.02* | - |
| 2.5 | 0.75 | 6 | Jan | - | - | - | *0.03* | - | *0.01* | - | - |
| 2.5 | 0.75 | 8 | Jan | - | - | - | *0.01* | - | - | - | - |

Table S6: Inclusion probabilities for the phylogeographic GLM comparison (C) of peak time between November-aggregated (Nov) and December-aggregated (Dec) fluxes based on a non-Markovian GLEAM parameterization. The highest inclusion probabilities for each data set are shown in bold,zero values in hyphen and non-zero rates in italic.

| $R_{max}$ | $R_{min}$ | D | C | $H3_{nr}$ | $H3_{r}$ | $H1_{nr}$ | $H1_{r}$ | $YAM_{nr}$ | $YAM_{r}$ | $VIC_{nr}$ | $VIC_{r}$ |
|---|---|---|---|---|---|---|---|---|---|---|---|
| (air) | (air) | (air) | (air) | - | - | - | **0.91** | - | *0.03* | *0.04* | **1.00** |
| 1.25 | 0.5 | 1 | Nov | - | - | - | - | - | - | - | - |
| 1.25 | 0.5 | 2 | Nov | - | - | - | - | - | - | - | - |
| 1.25 | 0.5 | 4 | Nov | - | - | - | - | - | - | - | - |
| 1.25 | 0.5 | 6 | Nov | - | - | - | - | - | - | - | - |
| 1.25 | 0.5 | 8 | Nov | - | - | - | - | - | - | - | - |

| | | | | | | | | | | | |
|---|---|---|---|---|---|---|---|---|---|---|---|
| 1.25 | 0.75 | 1 | Nov | - | - | - | - | - | - | - | - |
| 1.25 | 0.75 | 2 | Nov | - | - | - | - | - | - | - | - |
| 1.25 | 0.75 | 4 | Nov | - | - | - | - | - | - | - | - |
| 1.25 | 0.75 | 6 | Nov | - | - | - | - | - | - | - | - |
| 1.25 | 0.75 | 8 | Nov | - | - | - | - | - | - | - | - |
| 1.5 | 0.5 | 1 | Nov | - | - | - | - | - | - | - | - |
| 1.5 | 0.5 | 2 | Nov | - | - | - | - | - | - | - | - |
| 1.5 | 0.5 | 4 | Nov | - | - | - | - | - | - | - | - |
| 1.5 | 0.5 | 6 | Nov | - | - | - | - | - | - | - | - |
| 1.5 | 0.5 | 8 | Nov | - | - | - | - | - | - | - | - |
| 1.5 | 0.75 | 1 | Nov | - | - | - | - | - | - | - | - |
| 1.5 | 0.75 | 2 | Nov | - | - | - | - | - | - | - | - |
| 1.5 | 0.75 | 4 | Nov | - | - | - | - | - | - | - | - |
| 1.5 | 0.75 | 6 | Nov | - | - | - | - | - | - | - | - |
| 1.5 | 0.75 | 8 | Nov | - | - | - | - | - | - | - | - |
| 1.75 | 0.5 | 1 | Nov | - | - | - | - | - | - | - | - |
| 1.75 | 0.5 | 2 | Nov | - | - | - | - | - | - | - | - |
| 1.75 | 0.5 | 4 | Nov | - | - | - | - | - | - | - | - |
| 1.75 | 0.5 | 6 | Nov | - | - | - | - | - | - | - | - |
| 1.75 | 0.5 | 8 | Nov | - | - | - | - | - | - | - | - |
| 1.75 | 0.75 | 1 | Nov | - | - | - | - | - | - | - | - |
| 1.75 | 0.75 | 2 | Nov | - | - | - | - | - | - | - | - |
| 1.75 | 0.75 | 4 | Nov | - | - | - | - | - | - | - | - |
| 1.75 | 0.75 | 6 | Nov | - | - | - | - | - | - | - | - |
| 1.75 | 0.75 | 8 | Nov | - | - | - | - | - | - | - | - |
| 2 | 0.5 | 1 | Nov | - | - | - | - | - | - | - | - |
| 2 | 0.5 | 2 | Nov | - | - | - | - | - | - | - | - |
| 2 | 0.5 | 4 | Nov | - | - | - | - | - | - | - | - |
| 2 | 0.5 | 6 | Nov | - | - | - | - | - | - | - | - |
| 2 | 0.5 | 8 | Nov | - | - | - | - | - | - | - | - |
| 2 | 0.75 | 1 | Nov | - | - | - | - | - | - | *0.03* | - |
| 2 | 0.75 | 2 | Nov | - | - | - | - | - | - | - | - |
| 2 | 0.75 | 4 | Nov | - | - | - | - | - | - | - | - |
| 2 | 0.75 | 6 | Nov | - | - | - | - | - | - | - | - |
| 2 | 0.75 | 8 | Nov | - | - | - | - | - | - | - | - |
| 2.25 | 0.5 | 1 | Nov | - | - | - | - | - | - | *0.01* | - |
| 2.25 | 0.5 | 2 | Nov | - | - | - | - | - | - | - | - |
| 2.25 | 0.5 | 4 | Nov | - | - | - | - | - | - | - | - |
| 2.25 | 0.5 | 6 | Nov | - | - | - | - | - | - | - | - |
| 2.25 | 0.5 | 8 | Nov | - | - | - | - | - | - | - | - |

| | | | | | | | | | | | |
|---|---|---|---|---|---|---|---|---|---|---|---|
| 2.25 | 0.75 | 1 | Nov | - | *0.01* | - | - | - | - | *0.04* | - |
| 2.25 | 0.75 | 2 | Nov | - | - | - | - | - | - | - | - |
| 2.25 | 0.75 | 4 | Nov | - | - | - | - | - | - | - | - |
| 2.25 | 0.75 | 6 | Nov | - | - | - | - | - | - | - | - |
| 2.25 | 0.75 | 8 | Nov | - | - | - | - | - | - | - | - |
| 2.5 | 0.5 | 1 | Nov | - | - | - | - | - | - | - | - |
| 2.5 | 0.5 | 2 | Nov | - | - | - | - | - | - | - | - |
| 2.5 | 0.5 | 4 | Nov | - | - | - | - | - | - | - | - |
| 2.5 | 0.5 | 6 | Nov | - | - | - | - | - | - | - | - |
| 2.5 | 0.5 | 8 | Nov | - | - | - | - | - | - | - | - |
| 2.5 | 0.75 | 1 | Nov | - | *0.01* | - | - | - | *0.01* | *0.03* | - |
| 2.5 | 0.75 | 2 | Nov | - | - | - | - | - | - | - | - |
| 2.5 | 0.75 | 4 | Nov | - | - | - | - | - | *0.01* | - | - |
| 2.5 | 0.75 | 6 | Nov | - | - | - | - | - | - | - | - |
| 2.5 | 0.75 | 8 | Nov | - | - | - | - | - | - | - | - |
| 1.25 | 0.5 | 1 | Dec | - | - | - | - | - | - | - | - |
| 1.25 | 0.5 | 2 | Dec | - | - | - | - | - | - | - | - |
| 1.25 | 0.5 | 4 | Dec | - | - | - | - | - | - | - | - |
| 1.25 | 0.5 | 6 | Dec | - | - | - | - | - | - | - | - |
| 1.25 | 0.5 | 8 | Dec | - | - | - | - | - | - | - | - |
| 1.25 | 0.75 | 1 | Dec | - | - | **0.26** | - | - | - | - | - |
| 1.25 | 0.75 | 2 | Dec | - | - | *0.02* | - | - | - | - | - |
| 1.25 | 0.75 | 4 | Dec | - | - | - | - | - | - | - | - |
| 1.25 | 0.75 | 6 | Dec | - | - | - | - | - | - | - | - |
| 1.25 | 0.75 | 8 | Dec | - | - | - | - | - | - | - | - |
| 1.5 | 0.5 | 1 | Dec | - | - | - | - | - | - | - | - |
| 1.5 | 0.5 | 2 | Dec | - | - | - | - | - | - | - | - |
| 1.5 | 0.5 | 4 | Dec | - | - | - | - | - | - | - | - |
| 1.5 | 0.5 | 6 | Dec | - | - | - | - | - | - | - | - |
| 1.5 | 0.5 | 8 | Dec | - | - | - | - | - | - | - | - |
| 1.5 | 0.75 | 1 | Dec | **0.68** | **0.92** | *0.05* | *0.03* | - | *0.07* | **0.49** | - |
| 1.5 | 0.75 | 2 | Dec | **0.30** | *0.02* | *0.21* | *0.01* | *0.02* | *0.03* | *0.22* | - |
| 1.5 | 0.75 | 4 | Dec | - | - | - | - | *0.03* | *0.02* | - | - |
| 1.5 | 0.75 | 6 | Dec | - | - | *0.24* | - | *0.01* | *0.01* | - | - |
| 1.5 | 0.75 | 8 | Dec | - | - | *0.01* | - | - | - | - | - |
| 1.75 | 0.5 | 1 | Dec | - | - | - | - | - | - | - | - |
| 1.75 | 0.5 | 2 | Dec | - | - | - | - | - | - | - | - |
| 1.75 | 0.5 | 4 | Dec | - | - | - | - | - | *0.01* | - | - |
| 1.75 | 0.5 | 6 | Dec | - | - | - | - | - | - | - | - |
| 1.75 | 0.5 | 8 | Dec | - | - | - | - | - | - | - | - |

| | | | | | | | | | | | |
|---|---|---|---|---|---|---|---|---|---|---|---|
| 1.75 | 0.75 | 1 | Dec | - | - | - | - | - | - | - | - |
| 1.75 | 0.75 | 2 | Dec | - | - | - | - | *0.01* | *0.03* | *0.03* | - |
| 1.75 | 0.75 | 4 | Dec | *0.01* | *0.04* | *0.03* | *0.01* | *0.05* | *0.07* | *0.03* | - |
| 1.75 | 0.75 | 6 | Dec | - | - | *0.13* | *0.03* | *0.20* | *0.13* | - | - |
| 1.75 | 0.75 | 8 | Dec | - | - | *0.04* | *0.01* | *0.17* | *0.07* | - | - |
| 2 | 0.5 | 1 | Dec | - | - | - | - | - | - | - | - |
| 2 | 0.5 | 2 | Dec | - | - | - | - | - | - | - | - |
| 2 | 0.5 | 4 | Dec | - | - | - | - | - | - | - | - |
| 2 | 0.5 | 6 | Dec | - | - | - | - | - | - | - | - |
| 2 | 0.5 | 8 | Dec | - | - | - | - | *0.01* | *0.01* | - | - |
| 2 | 0.75 | 1 | Dec | - | - | - | - | - | - | - | - |
| 2 | 0.75 | 2 | Dec | - | - | - | - | - | *0.02* | *0.01* | - |
| 2 | 0.75 | 4 | Dec | - | - | - | - | - | *0.01* | *0.01* | - |
| 2 | 0.75 | 6 | Dec | - | - | - | - | *0.06* | *0.07* | *0.01* | - |
| 2 | 0.75 | 8 | Dec | - | - | - | - | *0.24* | *0.17* | - | - |
| 2.25 | 0.5 | 1 | Dec | - | - | - | - | - | - | - | - |
| 2.25 | 0.5 | 2 | Dec | - | - | - | - | - | - | - | - |
| 2.25 | 0.5 | 4 | Dec | - | - | - | - | - | - | - | - |
| 2.25 | 0.5 | 6 | Dec | - | - | - | - | - | - | - | - |
| 2.25 | 0.5 | 8 | Dec | - | - | - | - | - | - | - | - |
| 2.25 | 0.75 | 1 | Dec | - | - | - | - | - | - | - | - |
| 2.25 | 0.75 | 2 | Dec | - | - | - | - | - | *0.01* | *0.01* | - |
| 2.25 | 0.75 | 4 | Dec | - | - | - | - | *0.02* | *0.02* | - | - |
| 2.25 | 0.75 | 6 | Dec | *0.01* | - | - | - | *0.09* | *0.04* | *0.02* | - |
| 2.25 | 0.75 | 8 | Dec | - | - | - | - | *0.02* | *0.07* | - | - |
| 2.5 | 0.5 | 1 | Dec | - | - | - | - | - | - | - | - |
| 2.5 | 0.5 | 2 | Dec | - | - | - | - | - | - | - | - |
| 2.5 | 0.5 | 4 | Dec | - | - | - | - | *0.01* | *0.01* | - | - |
| 2.5 | 0.5 | 6 | Dec | - | - | - | - | - | - | - | - |
| 2.5 | 0.5 | 8 | Dec | - | - | - | - | - | - | - | - |
| 2.5 | 0.75 | 1 | Dec | - | - | - | - | - | - | - | - |
| 2.5 | 0.75 | 2 | Dec | - | - | - | - | - | - | - | - |
| 2.5 | 0.75 | 4 | Dec | - | - | - | - | *0.02* | *0.01* | - | - |
| 2.5 | 0.75 | 6 | Dec | - | - | - | - | - | - | - | - |
| 2.5 | 0.75 | 8 | Dec | - | - | - | - | - | *0.01* | - | - |

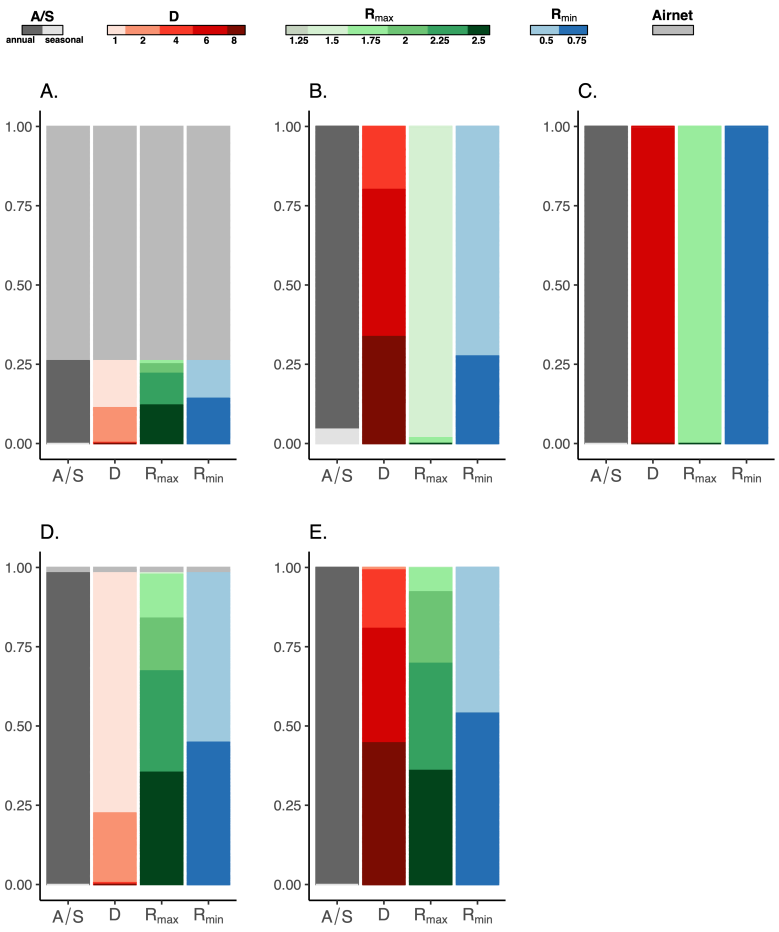


Figure S2: Marginal posterior inclusion probabilities associated with air travel fluxes and GLEAM fluxes for different simulations. 20 Replicates of discrete diffusion processes were simulated according to: (A) air travel; (B) annual GLEAM fluxes with Rmin=0.50, Rmax=1.5 and D=6 years; (C) annual GLEAM fluxes with Rmin=0.75, Rmax=1.75 and D=6 years; (D) annual GLEAM fluxes with Rmin=0.50, Rmax=2.25 and D=1 year, (D) annual GLEAM fluxes with Rmin=0.75, Rmax=2.50 and D=8 years. All GLEAM fluxes were based on a peak time in January. R = reproductive rate, D = waning of immunity, A/S = annual/seasonal.

## 4 Comparative analysis of simulated fluxes

We use a multidimensional scaling analysis (MDS) to explore the differences between the simulated travel fluxes resulting from different GLEAM parameterizations. We focus on how different parameterizations create different distributions of fluxes between April-September and October-March periods. To quantify these differences, first, we extract, for each parameterization, the matrix containing the difference between the two six-month periods (April-September and October-March), normalized by the total annual flux. Secondly, we compute the distance between matrices by summing the absolute differences between the individual elements. Finally, the MDS allows for visualizing these distances in a two-dimensional space. In Fig. S3, we compare, for each subtype and lineage, the fluxes generated by different values of waning of immunity and transmissibility peak while maintaining $R_{\max}$ constant at the value selected by the GLM. For all influenza subtypes and lineages, setting the peak of transmissibility in November and December leads to distributions between April-September and October-March fluxes that are more similar across waning of immunity values. On the other hand, when the peak of transmissibility is in January, the waning of immunity plays an important role in differentiating the flux distributions. For all influenza subtypes and lineages, the GLM consistently selects parametrizations that include the January peak and an immunity waning value that position best-supported parametrizations at one end of the data point cluster.

In Fig. S4, we compare different waning of immunity $D$ and $R_{\max}$ with peak of transmissibility for the northern hemisphere set at January 15th. Also, in this case, the parameterization selected by the GLM is the one positioned at one extreme of the cloud of points. Despite the fact that the flux distribution pattern varies in a complex way with the epidemiological parameters, the two analyses suggest that the GLM is able to capture a genuine signal in this variation.

## 5 Comparison simulated vs. observed epidemics

We compared simulated epidemics at the level of countries with available empirical records. Data on influenza laboratory-confirmed cases were obtained by FluNet [25], a free online database maintained by WHO since 1995. We used the FluNet weekly time series data limiting our analysis until 2019 to exclude the period heavily impacted by COVID-19. The H1N1pdm09 pandemic period (years 2009 and 2010) was also excluded. Furthermore,

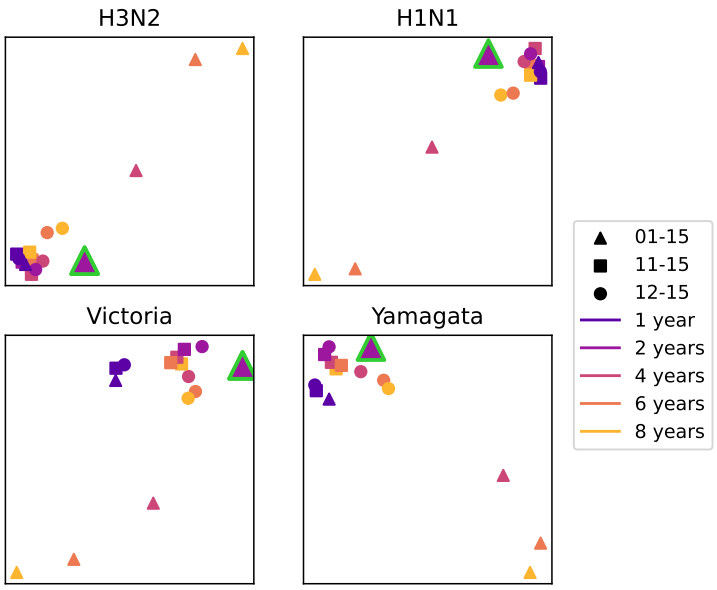


Figure S3: MDS plot illustrating flux differences for the selection of countries used for H3N2, H1N1, Yamagata, and Victoria lineages. Various symbols denote different peak transmissibility timings, while distinct colors represent the duration of waning of immunity. The green-highlighted symbol depicts the parameterization with the best support. We consider the best support parametrization obtained with a predictor based on the sample size residuals for H3N2, H1N1, and Yamagata. For Victoria, we employ the analysis without the sample size residual.

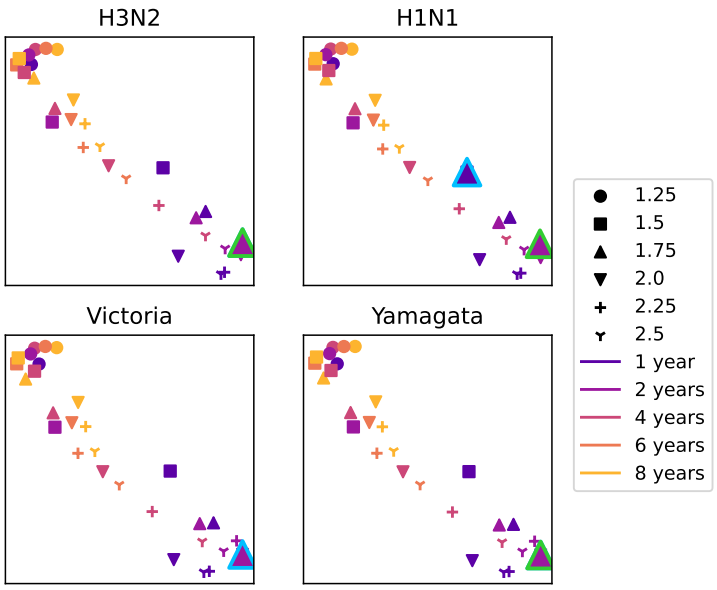


Figure S4: MDS plot illustrating flux differences for the selection of countries used for H3N2, H1N1, Yamagata, and Victoria lineages. Various symbols denote different values of $R_{\max}$, while distinct colors represent the duration of waning of immunity. We highlight the best support parametrization. For H3N2 and Yamagata, this is the same in the cases with and without sample size residuals (green border in the figure). For Victoria, we highlight the analysis without the sample size residuals (blue border). For H1N1, best support parametrizations differ in the cases with and without sample size residuals. These are both highlighted in the plot (green with sample size residuals, blue without).

Table S7: Number of countries used in the FluNet analysis, alongside the percentage relative to the total number of countries in the specified seasonal area.

| Region | H3N2 | H1N1 | YAM | VIC |
|---|---|---|---|---|
| Northern hemisphere | 64 (80%) | 36 (45%) | 34 (43%) | 28 (35%) |
| Southern hemisphere | 7 (64%) | 7 (64%) | 5 (45%) | 4 (36%) |
| Tropics | 54 (42%) | 19 (15%) | 30 (23%) | 25 (19%) |
| Worldwide | 125 (57%) | 62 (28%) | 69 (31%) | 57 (26%) |

we conducted subtype-specific analyses for distinct timeframes. Within influenza A subtype, we explored H3N2 from 1999 to 2019 and H1N1 from 1999 to 2008. Concerning influenza B lineages, our focus was on the period from 2011 to 2019, as limited data exists before 2011 concerning the differentiation between Victoria and Yamagata lineages. At the country level, the quality and coverage of the dataset have undergone changes over time. For each country we excluded seasons with less than two months of reported cases and retained only countries with data for at least three seasons. This led to a dataset comprising 125 countries for H3N2, 62 for H1N1, 69 for Yamagata, and 57 for Victoria. For clarity, we provide separate statistics for the three seasonal areas (northern hemisphere, southern hemisphere, and tropics). A country was categorized as northern (southern) hemisphere if 75% of its urban areas were located in that hemisphere and as tropics otherwise. For all subtypes and lineages, countries considered in the analysis were distributed in the three seasonal areas. However, distribution and coverage were highly heterogeneous, as summarized in Table S7.

Further, subtyping of influenza A isolates into e.g. H3N2 or H1N1 was not available in some instances. Thus, we adjusted H3N2 totals to account for untyped A isolates, by adding each month to H3N2 counts the factor $n_A \times n_{H3N2}/(n_{H3N2}+n_{H1N1}+n_{H1N1/09}+n_{H5N1})$, where $n_A$ is the number of untyped A isolates and $n_{H3N2}$, $n_{H1N1}$, $n_{H1N1/09}$ and $n_{H5N1}$ are the number of isolates for each subtype [26]. The same was done for H1N1 and for Victoria and Yamagata by considering the unsubtyped B data. From these records, we computed the monthly distribution of cases along the year for each year, and we averaged the profiles obtained in this way across the different seasons to obtain a single monthly distribution of incidence cases

Table S8: Spearman correlation coefficient between FluNet and simulated epidemics. We consider the best-supported parametrizations with residual for H3N2, H1N1, and Yamagata, and the best without residual for Victoria. The table reports the average correlation values over all countries for each seasonal area and worldwide. Average correlations are computed after the Fisher transformation.

| | H3N2 | H1N1 | YAM | VIC |
|---|---|---|---|---|
| Region | Av. corr. | Av. corr. | Av. corr. | Av. corr. |
| Northern hemisphere | 0.83±0.02 | 0.78±0.03 | 0.86±0.02 | 0.84±0.02 |
| Southern hemisphere | 0.66±0.08 | 0.52±0.09 | 0.79±0.03 | 0.68±0.04 |
| Tropics | 0.10±0.06 | 0.10±0.10 | 0.12±0.09 | 0.16±0.09 |
| Worldwide | 0.60±0.04 | 0.60±0.05 | 0.64±0.05 | 0.62±0.06 |

capturing robust features of the influenza epidemics of the country. We then compared these profiles with the same quantity as recovered from the simulations.

We consider the best support parametrization obtained with a predictor based on the sample size residuals for H3N2, H1N1, and Yamagata. For Victoria, we employ the analysis without sample size residual, as that GLEAM fluxes are not supported in analyses that include sample size residuals. The visual comparison between data and simulations is shown in Fig. 3 of the main paper for H3N2. In tropical countries, data are quite noisy. The model reproduces a rather flat average profile as model output is the result of averaging out oscillations in incidence which are driven by waning of immunity and whose period is not a multiple of the year. For the other countries, seasonal peaks of data and simulations are similar in the majority of cases - see below for a more in-depth discussion. For each subtype and lineage, average Spearman correlation coefficients broken down by seasonal area are reported in Table S8.

We then tested how model performance in reproducing FluNet epidemic profiles varies across epidemiological parameters. For $R_{\min} = 0.75$ and each subtype and lineage, the bar plots of Fig. S5 summarize the average correlation, computed over all countries varying $R_{\max}$ and $D$. The majority of scenarios tested show lower correlation compared to the best-supported parametrization. A few scenarios had a slightly higher correlation. Still, they were within the standard error of the best-supported parametrization.

Therefore, the parametrization selected by the GLM is among the ones that best reproduce incidence data.

Averages were taken over all countries of each region, combining the ones where genetic data were available for calibration (in-sample countries) with the ones where no genetic data were available (out-of-sample). Considering the best-support parametrization, and taking the average over each of the two groups separately we found for all subtypes and lineages no statistically significant difference between the two groups when averaging over all countries worldwide (Welch's t-test, with a significance threshold of $p = 0.05$). Breaking down countries by seasonal area, statistically significant differences were observed only for H1N1 and H3N2, when averaging over the northern hemisphere. For H3N2, the average correlations were $0.86 \pm 0.02$ and $0.78 \pm 0.02$ for the in-sample and out-of-sample groups, respectively, while the corresponding values for H1N1 were $0.81 \pm 0.03$ and $0.67 \pm 0.04$. Overall, the good values of correlation for out-of-sample countries demonstrate the model's capacity to capture robust influenza characteristics consistently across the two groups.

Beyond average correlation, we used lagged correlation to systematically analyze how well the best-support parametrization reproduced the time of epidemic peaks in each country. For each country and subtype/lineage, we systematically explored all possible time lags in months between simulations and data to identify the optimal lag that maximizes the Spearman correlation. Taking the average over all countries worldwide, the optimal lag was close to zero for all subtypes/lineages (-0.35, -0.57, 0.49, and 0.44 months for H3N2, H1N1, Yamagata and Victoria, respectively). This confirms that the parametrization selected by the GLM well captured global trends. Still, looking at individual countries revealed variations that were not always captured by the model, especially in the tropics. More precisely, the optimal lag was between -1 and 1 months in the majority of countries in the northern and southern hemispheres - 83% to 93% of countries in the northern hemisphere and 57% to 100% of countries in the southern hemisphere according to the subtype/lineage. However, it was within the same range for only 16% to 30% of countries in the tropics, according to the subtype/lineage. This highlights that variations across countries in peak seasonality are essential ingredients to be accounted for in future, more refined versions of the model.

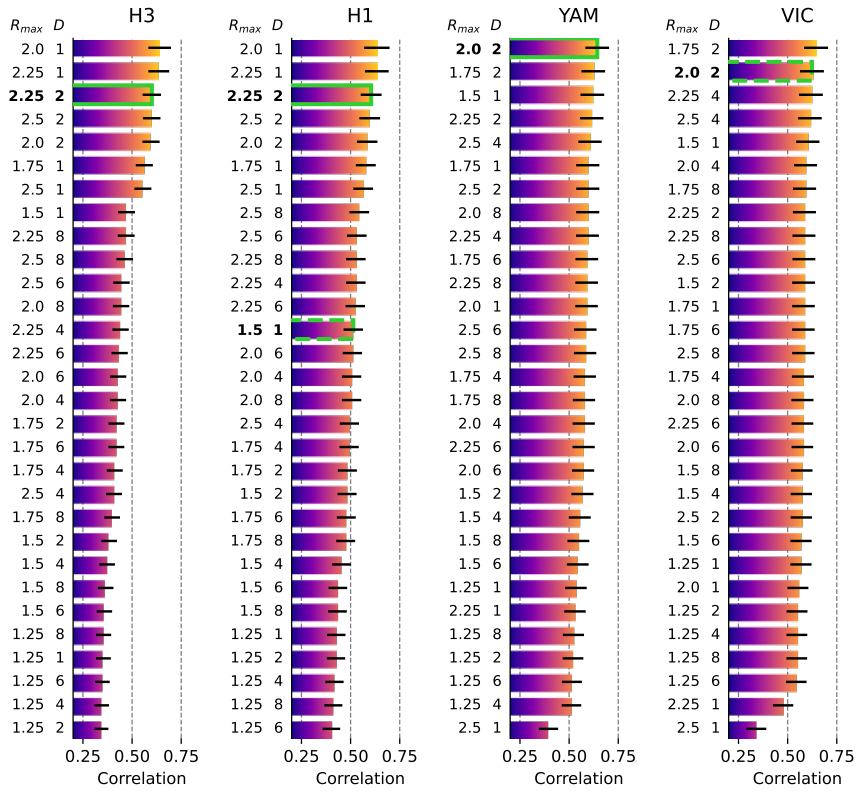


Figure S5: For each influenza subtype and lineage, the figure displays the worldwide average Spearman correlation between FluNet profiles and the simulated incidence computed as in Table S8. The parameterization receiving the highest support is highlighted in green. For H1N1, since the parametrizations with and without residuals differ, the best parametrization with residuals is highlighted with a continuous line, while the one without residual is highlighted with a dashed line. In case of Victoria, only the parametrization without residual is highlighted since, with residual no GLEAM parametrizations outperform air-travel. The error bars display the standard error.

# 6 Influenza migration patterns

In Tables S10 and S9, we display the average migration fluxes among the selected regions shown in Fig. 4, obtained from the GLEAM simulation for the two epochs. Note that only dominant fluxes are displayed in Fig. 4, while all fluxes are reported in the tables. Colormaps representing the two tables are displayed in Fig. S6.

Table S9: Simulated fluxes of imported cases among the regions used in Fig 4 of the main text, for the April-September period. Results for the scenario selected by GLM for H3N2, i.e. $R_{\max} = 2.25$, $R_{\min} = 0.75$ and $D = 2$ years.

| From<br><br>To | New Zealand and Australia | Latin America | India | South Korea and Japan | Europe | North China | Southeast Asia | South China | North America |
|---|---|---|---|---|---|---|---|---|---|
| New Zealand and Australia | 0 | 164 | 298 | 170 | 405 | 131 | 3274 | 565 | 252 |
| Latin America | 171 | 0 | 15 | 27 | 792 | 19 | 46 | 60 | 1149 |
| India | 638 | 32 | 0 | 53 | 346 | 31 | 2732 | 311 | 291 |
| South Korea and Japan | 1040 | 157 | 167 | 0 | 305 | 549 | 5900 | 1921 | 367 |
| Europe | 2589 | 4496 | 1261 | 325 | 0 | 236 | 3869 | 775 | 2382 |
| North China | 858 | 115 | 114 | 640 | 229 | 0 | 2814 | 22188 | 226 |
| Southeast Asia | 4870 | 64 | 2141 | 1236 | 775 | 558 | 0 | 4785 | 262 |
| South China | 1211 | 113 | 280 | 756 | 216 | 6354 | 7761 | 0 | 232 |
| North America | 1463 | 6227 | 1043 | 341 | 2039 | 192 | 1194 | 664 | 0 |

Table S10: Simulated fluxes of imported cases among the regions used in Fig 4 of the main text, for the October-March period. Results for the scenario selected by GLM for H3N2, i.e. $R_{\max} = 2.25$, $R_{\min} = 0.75$ and $D = 2$ years.

| From<br>To | New Zealand and Australia | Latin America | India | South Korea and Japan | Europe | North China | Southeast Asia | South China | North America |
|---|---|---|---|---|---|---|---|---|---|
| New Zealand and Australia | 0 | 28 | 487 | 1035 | 2468 | 850 | 3172 | 1003 | 1428 |
| Latin America | 12 | 0 | 28 | 181 | 5604 | 138 | 47 | 112 | 8734 |
| India | 81 | 10 | 0 | 558 | 3659 | 356 | 3456 | 722 | 2615 |
| South Korea and Japan | 224 | 68 | 493 | 0 | 4349 | 8805 | 7924 | 8824 | 4481 |
| Europe | 395 | 2754 | 3142 | 4331 | 0 | 3539 | 5349 | 2233 | 28913 |
| North China | 131 | 53 | 310 | 8666 | 3552 | 0 | 4068 | 71975 | 2869 |
| Southeast Asia | 594 | 19 | 3650 | 10217 | 6785 | 5136 | 0 | 11799 | 2030 |
| South China | 171 | 49 | 684 | 8897 | 2335 | 78533 | 9661 | 0 | 2360 |
| North America | 237 | 4946 | 2225 | 4537 | 29456 | 2914 | 1560 | 2308 | 0 |

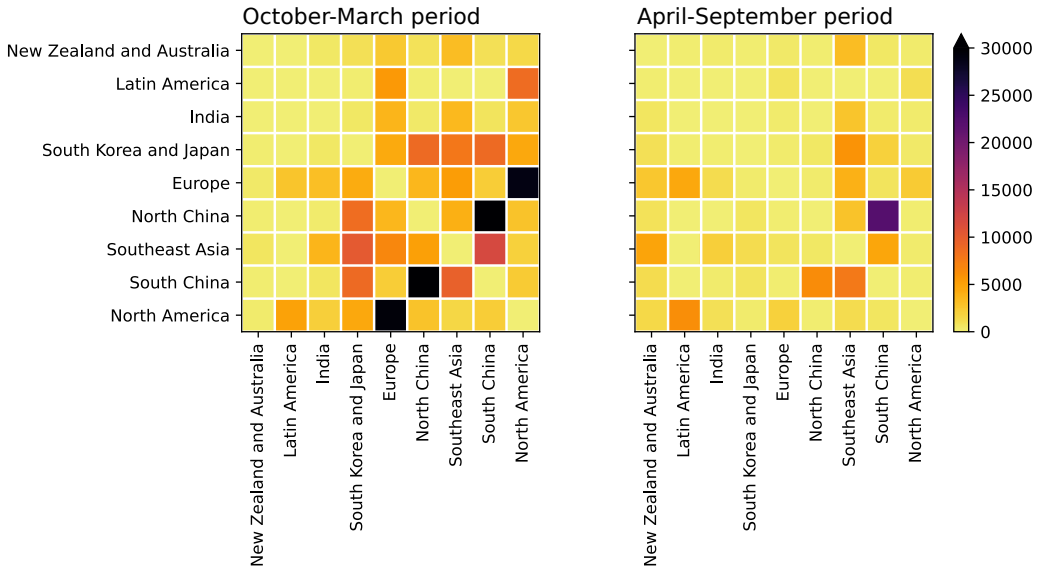


Figure S6: Simulated fluxes of imported cases among the regions used in Fig 4 of the main text. Results for the scenario selected by GLM for H3N2, i.e. $R_{\max} = 2.25$, $R_{\min} = 0.75$ and $D = 2$ years.

## References


[1] "Center for International Earth Science Information Network (CIESIN), Columbia University; and Centro Internacional de Agricultura Tropical (CIAT). The Gridded Population of the World Version 3 (GPWv3): Population Grids. Palisades, NY: Socioeconomic Data and Applications Center (SEDAC), Columbia University."

[2] "International Air Transport Association (IATA)."

[3] D. Balcan, V. Colizza, B. Gonçalves, H. Hu, J. J. Ramasco, and A. Vespignani, "Multiscale mobility networks and the spatial spreading of infectious diseases," *Proceedings of the national academy of sciences*, vol. 106, no. 51, pp. 21484–21489, 2009.

[4] D. Balcan, H. Hu, B. Goncalves, P. Bajardi, C. Poletto, J. J. Ramasco, D. Paolotti, N. Perra, M. Tizzoni, V. d. W. Broeck, V. Colizza, and A. Vespignani, "Seasonal transmission potential and activity peaks of the new influenza A(H1n1): a Monte Carlo likelihood analysis based on human mobility," *BMC Medicine*, vol. 7, p. 45, 2009.

[5] M. A. Serrano, M. Boguñá, and A. Vespignani, "Extracting the multiscale backbone of complex weighted networks," *Proceedings of the National Academy of Sciences of the United States of America*, vol. 106, pp. 6483–6488, Apr. 2009.

[6] M. E. Halloran, I. M. L. Jr, and C. J. Struchiner, "Binomial and Stochastic Transmission Models," in *Design and Analysis of Vaccine Studies*, Statistics for Biology and Health, pp. 63–84, Springer New York, 2010. DOI: 10.1007/978-0-387-68636-3_4.

[7] L. Sattenspiel and K. Dietz, "A structured epidemic model incorporating geographic mobility among regions," *Mathematical Biosciences*, vol. 128, pp. 71–91, Aug. 1995.

[8] M. J. Keeling and P. Rohani, "Estimating spatial coupling in epidemiological systems: a mechanistic approach," *Ecology Letters*, vol. 5, pp. 20–29, Jan. 2002.

[9] D. Balcan and A. Vespignani, "Phase transitions in contagion processes mediated by recurrent mobility patterns," *Nature Physics*, vol. 7, pp. 581–586, July 2011.

[10] C. Poletto, M. Tizzoni, and V. Colizza, "Heterogeneous length of stay of hosts' movements and spatial epidemic spread," *Scientific reports*, vol. 2, no. 1, p. 476, 2012.

[11] D. Balcan, H. Hu, B. Goncalves, P. Bajardi, C. Poletto, J. J. Ramasco, D. Paolotti, N. Perra, M. Tizzoni, W. Van den Broeck, *et al.*, "Seasonal transmission potential and activity peaks of the new influenza a (h1n1): a monte carlo likelihood analysis based on human mobility," *BMC medicine*, vol. 7, pp. 1–12, 2009.

[12] P. Bajardi, C. Poletto, J. J. Ramasco, M. Tizzoni, V. Colizza, and A. Vespignani, "Human mobility networks, travel restrictions, and the global spread of 2009 h1n1 pandemic," *PloS one*, vol. 6, no. 1, p. e16591, 2011.

[13] B. S. Cooper, R. J. Pitman, W. J. Edmunds, and N. J. Gay, "Delaying the International Spread of Pandemic Influenza," *PLOS Med*, vol. 3, p. e212, May 2006.

[14] M. Biggerstaff, S. Cauchemez, C. Reed, M. Gambhir, and L. Finelli, "Estimates of the reproduction number for seasonal, pandemic, and zoonotic influenza: a systematic review of the literature," *BMC infectious diseases*, vol. 14, no. 1, pp. 1–20, 2014.

[15] Z. P. Ross, N. Komadina, Y.-M. Deng, N. Spirason, H. A. Kelly, S. G. Sullivan, I. G. Barr, and E. C. Holmes, "Inter-Seasonal Influenza is Characterized by Extended Virus Transmission and Persistence," *PLOS Pathogens*, vol. 11, p. e1004991, June 2015.

[16] D. He, R. Lui, L. Wang, C. K. Tse, L. Yang, and L. Stone, "Global Spatio-temporal Patterns of Influenza in the Post-pandemic Era," *Scientific Reports*, vol. 5, p. 11013, June 2015.

[17] I. Dorigatti, S. Cauchemez, and N. M. Ferguson, "Increased transmissibility explains the third wave of infection by the 2009 H1N1 pandemic virus in England," *Proceedings of the National Academy of Sciences*, vol. 110, pp. 13422–13427, Aug. 2013. Publisher: Proceedings of the National Academy of Sciences.

[18] J. B. Axelsen, R. Yaari, B. T. Grenfell, and L. Stone, "Multiannual forecasting of seasonal influenza dynamics reveals climatic and evolutionary drivers," *Proceedings of the National Academy of Sciences*, vol. 111, pp. 9538–9542, July 2014.

[19] J. Truscott, C. Fraser, S. Cauchemez, A. Meeyai, W. Hinsley, C. A. Donnelly, A. Ghani, and N. Ferguson, "Essential epidemiological mechanisms underpinning the transmission dynamics of seasonal influenza," *Journal of The Royal Society Interface*, p. rsif20110309, June 2011.

[20] P. Lemey, A. Rambaut, T. Bedford, N. Faria, F. Bielejec, G. Baele, C. A. Russell, D. J. Smith, O. G. Pybus, D. Brockmann, and M. A. Suchard, "Unifying Viral Genetics and Human Transportation Data to Predict the Global Transmission Dynamics of Human Influenza H3n2," *PLoS Pathog*, vol. 10, p. e1003932, Feb. 2014.

[21] F. Bielejec, P. Lemey, G. Baele, A. Rambaut, and M. A. Suchard, "Inferring heterogeneous evolutionary processes through time: from sequence substitution to phylogeography," *Syst. Biol.*, vol. 63, pp. 493–504, Jul 2014.

[22] M. A. Suchard, P. Lemey, G. Baele, D. L. Ayres, A. J. Drummond, and A. Rambaut, "Bayesian phylogenetic and phylodynamic data integration using beast 1.10," *Virus Evolution*, vol. 4, no. 1, p. vey016, 2018.

[23] D. Ayres, M. Cummings, G. Baele, A. Darling, P. Lewis, J. Huelsenbeck, P. Lemey, A. Rambaut, and M. Suchard, "BEAGLE 3.0: Improved usability for a high-performance computing library for statistical phylogenetics," *Systematic Biology*, vol. 68, p. 1052–1061, 2019.

[24] F. Bielejec, P. Lemey, L. M. Carvalho, G. Baele, A. Rambaut, and M. A. Suchard, "$\pi$buss: a parallel beast/beagle utility for sequence simulation under complex evolutionary scenarios," *BMC Bioinformatics*, vol. 15, no. 133, 2014.

[25] N. I. C. N. of the Global Influenza Surveillance and Response System (GISRS) and World Health OrganisationWHO, "FluNet."

[26] B. S. Finkelman, C. Viboud, K. Koelle, M. J. Ferrari, N. Bharti, and B. T. Grenfell, "Global Patterns in Seasonal Activity of Influenza A/H3n2, A/H1n1, and B from 1997 to 2005: Viral Coexistence and Latitudinal Gradients," *PLoS ONE*, vol. 2, p. e1296, Dec. 2007.